Biochemical and Biophysical Research Communications **283,** 48–56 (2001)
doi:10.1006/bbrc.2001.4741, available online at http://www.idealibrary.com on IDEAL®

Human Septin 3 on Chromosome 22q13.2 Is Upregulated by Neuronal Differentiation

Axel Methner,[1] Frank Leypoldt, Patrick Joost, and Jan Lewerenz
Department of Neurology and Zentrum für Molekulare Neurobiologie, University Hospital Hamburg, Falkenried 94, D-20251 Hamburg, Germany

Received March 13, 2001

An expression sequence tag identified in a screen for genes upregulated by retinoic acid induced neuronal differentiation of the human teratocarcinoma cell line Ntera2/D1 was found in close genomic proximity to a region of high sequence homology to the septin subfamily of GTPase genes. We could show that the tag corresponds to the 3′ untranslated region of this novel gene named septin 3 and cloned three isoforms A (2191 bp), B (4378 bp), and C (1896 bp) from human Ntera2/D1 cDNA. We present the genomic localization and organization on chromosome 22q13.2, a chromosomal hot spot for translocations implicated in leukemia. Interestingly, MSF the closest paralog of septin 3 is a fusion partner in a therapy-related acute myeloid leukemia. Quantitative PCR confirmed the upregulation of the putative septin by neuronal differentiation and northern blotting showed only one band corresponding to sep3B with a neurospecific expression pattern in adult human tissues. © 2001 Academic Press

Key Words: **Ntera2cl.D/1 (NT2) cells; neuronal differentiation; septin; leukemia.**

Neurons and glia derive from pluripotent precursor cells and differentiate in response to environmental and intrinsic factors. This process can be studied *in vitro* by retinoic acid (RA) induced differentiation of the human teratocarcinoma cell line NTera-2/D1 (NT2). NT2 cells remain as undifferentiated mitotic precursor cells, when maintained under defined tissue culture conditions. Upon exposure to RA and the use of differential adhesion matrices and mitotic inhibitors, the cells develop the morphological and cytoskeletal characteristics of postmitotic central nervous system (CNS) neurons (1). This seems to model the *in vivo* situation, as high concentrations of RA have been detected in the embryonic CNS and the developing spinal cord (2–4). RA binding proteins and its receptors are present in the developing nervous system suggesting a role in neurogenesis (5–8).

A screen for genes regulated by RA-induced differentiation of NT2 cells generated I-U#19, an expressed sequence tag (EST) with no homology to known genes (9). The progress of the human genome project assigned this EST to human chromosome 22q13.2 in close genomic proximity to a region of high sequence homology to the septin subfamily of GTPase genes. This putative gene shares strong similarity to the mouse neuronal-specific septin 3 (10) and rat brain-specific G-septin (11). The septins are a family of 40–50 kDa GTPases that were first identified in *Saccharomyces cerevesiae* as proteins required for the completion of the cell cycle (12). These proteins share several characteristics, e.g., a P-loop nucleotide-binding consensus sequence for GTP binding near the N terminus (13), and most are predicted to have a coiled-coil domain at the C terminus. Mutations of yeast septins lead to the disruption of a characteristic set of filaments associated with the plasma membrane and result in cell cycle arrest and defective cytokinesis (14). Yeast septins form hetero-oligomeric filaments that contribute to bud site selection and neck stability (reviewed in (15)). Septin proteins from Drosophila also assemble into hetero-oligomeric filaments (16) and are required for cytokinesis (17). The mammalian septin NEDD5 localizes near the contractile ring during cytokinesis in HeLa cells, and microinjection of anti-NEDD5 antibodies into dividing cells results in binucleated cells, suggesting that NEDD5 plays an essential role during cytokinesis (18). New roles for neuronal septins are emerging in synaptic transmission neurons (19). Other septin genes known in mammalian tissues are mouse DIFF6 (20), mouse PNUTL2/H5 (21), human CDC10 (22), human CDCrel-1/PNUTL1 (23, 24), human SEP2-like (25), human SEPTIN 6 (26), human MSF/mouse SINT1 (27, 28).

In this study, we used the sequence information from I-U#19 to clone a novel human septin with high homology to mouse neuronal-specific septin 3 and rat

[1] To whom correspondence should be addressed. Fax: +49 40 4 28 03 51 01. E-mail: methner@uke.uni-hamburg.de.

0006-291X/01 $35.00

G-septin from cDNA derived from RA-induced NT2 cells. We could determine its genomic location and structure, and show that this gene is upregulated by RA-induced neuronal differentiation of NT2 cells, and that its expression is neurospecific in adult human tissues.

MATERIALS AND METHODS

Cell culture. NT2 cells were cultured and differentiated as previously described (9, 29). Briefly, cells were maintained in OptiMEM (Life Technologies) supplemented with 5% fetal calf serum (FCS, Linaris), 500 IU/ml penicillin and 500 μg/ml streptomycin (P/S). For aggregation, cells were dislodged by trypsinization and 10^6 cells/ml plated into 140-mm bacteriological grade petri dishes in 50 ml DMEM-HG (high glucose) with 10% FCS and P/S. After overnight incubation at 37°C in a 5% CO_2 incubator the aggregates were treated with 1 μM all trans-RA. Medium and culture dish were replaced every three days. After 21 days of RA treatment, the aggregates were plated onto tissue culture grade petri dishes or coverslips, precoated with 10 μg/ml poly-D-lysine (Sigma) and 10 μg/ml mouse laminin (Sigma) in DMEM-HG with 10% FCS and P/S supplemented with 10 μg/ml cytosin-D-arabinofuranosid (Sigma) und 1 μg/ml uridine (Sigma) for 7 days. Medium was replaced once after 4 days. Cells were harvested after an additional day without cytosin-D-arabinofuranosid and used for RNA preparation and further characterization by immunocytochemistry.

Immunocytochemistry. We performed immunocytochemistry on differentiated and undifferentiated NT2 cultures using a monoclonal rabbit anti-human neurofilament H (NF-H) IgG antibody (Serotec, 1:1000), a monoclonal rabbit anti-human glial fibrillary acidic protein (GFAP) IgG antibody (Boehringer, 1:500) and a monoclonal mouse anti-human highly phosphorylated NF-M IgG antibody (Zymed, 1:200). Secondary antibodies were a polyclonal alkaline phosphatase (AP)-conjugated goat anti-mouse IgG (Sigma, 1:7000) and a polyclonal AP-conjugated goat anti-rabbit IgG (Promega, 1:7000). The cultures were plated on coverslips and fixed with a solution containing 4% formaldehyde, 7% acetic acid, and 7% glycerol in H_2O for 1 h and washed twice for 10 min with 0.05% Triton 100 in phosphate buffered saline. The coverslips were then incubated with the primary antibodies followed by AP-conjugated secondary antibodies and the AP-substrates 133 μg/ml 5-bromo-4-chloro-3-indolylphosphat and 266 μg/ml nitrobluetetrazolium. The reaction was stopped with 25 mM Tris–HCl pH 8.0 and 10 mM EDTA pH 8.0. After drying the coverslips were mounted in glycerol.

mRNA isolation and cDNA synthesis. Approximately 2×10^8 differentiated and undifferentiated cells were used for total RNA extraction using the TRIzol reagent (GibcoBRL) and poly-$(A)^+$ RNA purified with two rounds of DynaBeads (Dynal). Approximately 1 μg poly-$(A)^+$ RNA was reverse transcribed with MMLV reverse transcriptase (Promega) and oligo-$(dT)^{15}$ primers.

Isolation of transcript sequences and analysis of genomic sequences. The sequence information derived from I-U#19 (9) was used to assemble all publicly available EST sequences into a virtual transcript (http://www.ncbi.nlm.nih.gov/BLAST/thcblast.html). This sequence THC365960 was compared to the genomic subset of GenBank by Advanced Blast 2.0 (http://www.ncbi.nlm.nih.gov/cgi-bin/BLAST/) (30) and identified a human DNA sequence from clone CTA-250D10 on chromosome 22 (Accession No. z99716) downstream from a gene similar to mouse neuronal-specific septin 3. PCR primer R1 (5′-AAGAGCGTGTTGACCAGCGTTGAT-3′) was constructed from the genomic sequence corresponding to the 5′ end of the translated sequence and used with the vector-specific primer m13 forward (5′-GCTATTACGCCAGCTGGCGAAAGGGGGATGTG-3′) to amplify the missing 5′ end from a human GeneFinder cDNA pool containing 200832 clones from caudate nucleus, thymus, pericardium, pituitary gland, adult brain, thalamus, spleen and amygdala obtained from the German Resource Center (http://www.rzpd.de). Conditions were 94°C 10 s, 57°C 30 s, and elongation at 72°C 90 s for 40 cycles. An aliquot of the PCR reaction was cloned into the pCR2.1-TOPO vector (Invitrogen) and transformed into DH5α competent cells. Ninety-six clones were dot-blotted onto a nylon membrane (Porablot, Machery and Nagel) and hybridized to the end-labeled oligonucleotide F2 (5′-AGAGTGGACTGGGCAAATC-3′) located immediately upstream from R1 to identify specific products. The blot was washed under high stringency conditions and exposed to a phosphoimaging system (Fujix) for 30 min. Four hybridizing clones containing inserts between 238 and 260 bp were sequenced by the dideoxy chain termination method using an Applied Biosystems automated DNA sequencer. PCR primer F1 (5′-CGGGACAAAGGAGGATTC-3′) was constructed from the 5′ end of the longest insert and used with R3 (5′-TCACCGTAAGATTGGCTGGGACTG-3′) from I-U#19 to amplify the presumed gene by PCR from cDNA derived from differentiated NT2-cells. Conditions were 94°C 10 s, 57°C 30 s, and elongation at 72°C 4 min for 10 cycles and 94°C 10 s, 57°C 30 s, and 72°C 4 min (+10 s per cycle) for additional 25 cycles. An aliquot was run on a 2% agarose gel (SeaKerm LE Agarose, FMC BioProducts), alkaline blotted onto a nylon membrane (Porablot, Machery & Nagel) and hybridized to the end-labeled oligonucleotide R2 (5′-GTGGGGCAGTGGCAGTCAACATT-3′) from I-U#19 to identify specific amplification products. The blot was washed under high stringency conditions and exposed to a phosphoimaging system (Fujix) for 30 min. Hybridizing bands were excized, cloned into the pCR2.1-TOPO vector (Invitrogen) and sequenced. Exonic sequences were determined by aligning the cDNA with the genomic sequences. Exon/Intron boundaries were defined according to the consensus sequences given by Horowitz and Krainer (31).

Phylogenetic analysis. Amino acid sequences of all available mammalian septins were aligned with CLUSTALW 1.81 (32) using the protein weight matrix BLOSUM 30 with a gap open penalty of 10 and a gap extension penalty of 0.1. This parameters allow a slow, but accurate alignment. In cases where the human ortholog was not yet identified, the murine counterpart was used. Sequences used were human peanut-like protein 1 (Accession No. Q99719; alternative name; CDCREL-1), human peanut-like protein 2 (Accession No. O43236; alternative name, brain protein H5), human CDC10 protein homolog (Accession No. Q16181), human MLL septin-like fusion protein MSF-A (Accession No. AAF23374), human septin 2-like cell division control protein (Accession No. AAF67469), mouse DIFF6 (Accession No. P42209), mouse neural precursor cell expressed, developmentally down-regulated gene 5 (NEDD5, Accession No. NP_035021 and mouse septin6 (Accession No. BAA82838). A phylogenetic tree was inferred from the multiple sequence alignment by calculating maximum likelihood distances with Puzzle 5.0 (33) (http://www.tree-puzzle.de). The distances were corrected by the JTT substitution frequency matrix (34) with the amino acid usage and the shape parameter estimated from the data and the site-to-site rate variation modeled on a gamma distribution with eight rate categories plus invariant sites. Quartet puzzling trees were constructed using the described settings and 1000 puzzling steps to obtain support values for each internal branch.

Quantitative (RT)-PCR. Quantitative RT-PCR using the F3 (5′-CTCCTACCCCCAACCCCCTTCC-3′) and the R3 primer was performed on cDNA from differentiated and undifferentiated NT2-cells to confirm the induction of I-U#19 by retinoic acid. The cDNA was normalized for glyceraldehyde 3-phosphate dehydrogenase (gapdh) expression by PCR using forward primer (5′-ACCACAGTCCATGCCATCAC-3′) and reverse primer (5′-TCCACCACCCTGTTGCTGTA-3′). In order to roughly determine the exponential phase of amplification, aliquots of the PCR-reaction were removed after 15, 20, 25, 30, 35, and 40 cycles and checked on ethidium bromide stained agarose gels. PCR reactions were performed with either gapdh- or I-U#19-specific primer pairs alone or together in a multiplex reaction for both templates. All results were reproduced three

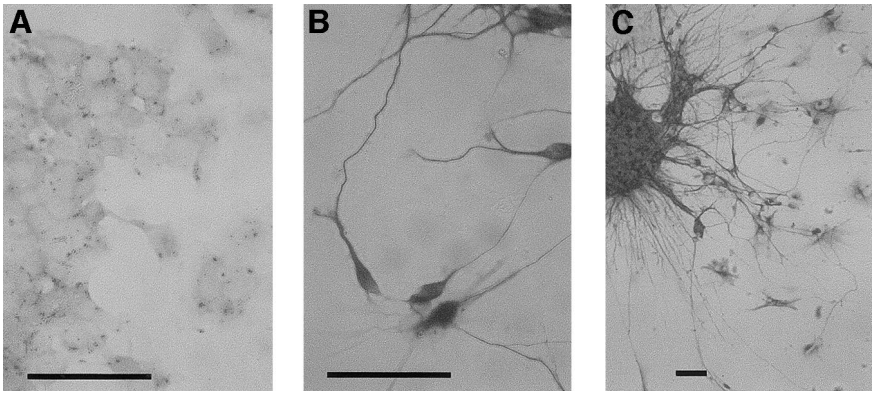

FIG. 1. Retinoic acid induced morphological and cytoskeletal changes of NT2 cells. Bright-field photomicrographs of cells stained with the late neuronal marker neurofilament H. Scale bar represents 100 μm. (A) Uninduced NT2 cells show no visible staining for neurofilament H. (B) Induced cells possess a conical cell body with long and thin interconnected extensions. The cell bodies and most extensions of induced cells are stained by antibodies against neurofilament H. (C) Aggregates of induced cells at day 8 after replating show migrated cell clusters and axons protruding directly from the aggregates all heavily stained by antibodies against neurofilament H.

times. Aliquots were removed every other round of amplification starting at the previously estimated cycle number of the start of linear amplification. Aliquots were run on a 2% agarose gel (SeaKem LE Agarose, FMC BioProducts) and alkaline blotted onto a nylon membrane (Porablot, Machery & Nagel). A gapdh-specific oligonucleotide (5′-GGATGACCTTGCCCACAGC-3′) and R2 were end-labeled and hybridized with the membranes overnight at 42°C. Specific activity was $>10^7$ cpm/pmol oligonucleotide. Membranes were washed under high-stringency conditions and exposed to a phosphoimaging system (Fujix) for various exposure times.

Autoradiographies were analysed using Tina Version 2.10 h (Raytest). A density profile (not shown) was created for each lane in the autoradiography (e.g., Fig. 5A). The baseline was estimated and subtracted from all values. The area under the curve for each band was determined and plotted on a semi-logarithmic scale against the cycle number for each reaction (Figs. 5B and 5C). All values were presumed to be valid when compared curves were parallel at a given cycle number, indicating both reactions still being in the exponential phase of amplification. Valid data were normalized to corresponding gapdh optical density. The mean, standard deviation and standard error of ratios of normalized optical density of amplification products from differentiated compared to undifferentiated templates was calculated and Student's ratio paired t-test performed to determine the significance.

Northern analysis. A human multiple tissue Northern blot was purchased from Clontech laboratories. A specific I-U#19 probe was generated by linear PCR in the presence of α-32P dATP (50 μCi) using the R2 primer and 25 ng I-U#19 template. Cycle parameters were 94°C 2 min, 57°C 2 min and 72°C 5 min for 30 cycles. Specific activity was $>10^7$ cpm/μg DNA. The blots were hybridized overnight in UltraHyb (Ambion) solution at 42°C and washed twice in 2× SSC and 0.1% sodium dodecyl sulfate (SDS) at 42°C for 10 min, and twice in 0.1× SSC and 0.1% SDS at 42°C for 15 min. Autoradiography was performed using a phosphoimaging system (Fujix) for 4 h.

RESULTS AND DISCUSSION

Induction of NT2 Cells

NT2 cells were induced by a method combining cell aggregation and induction by retinoic acid (29). Our induced NT2 cultures consist of the cell aggregates and postmitotic CNS-like neurons as judged by their morphology and the expression of late neuronal markers like phosphorylated neurofilaments M and H (Fig. 1). An antibody against glial fibrillary acidic protein did not stain the induced NT2 cultures suggesting the absence or at least underrepresentation of glial-like cells (not shown). The importance of cell aggregation in initiating neuronal differentiation has been reported in other cell types, such as embryonic stem cells and P19 cells (35, 36). We therefore did not separate the aggregates from migrated neuronal cells, assuming that cells with altered expression would probably also reside in these cell aggregates and used the cells to prepare mRNA and cDNA.

Cloning of Human Septin 3

The progress of the human genome project assigned I-U#19, a cDNA found by a screen for RA-induced genes, to a human DNA sequence from clone CTA-250D10 on chromosome 22 (GenBank Accession No. z99716) in the presumed 3′ untranslated region of a gene similar to

FIG. 2. Structural characteristics of mammalian septin 3 homologs. (A) Alignement of human SEP3A, B, and C, mouse SEP3 and rat G-SEPTIN A. Identical residues are shaded in black, similar residues in grey. Possible translational start sites are numbered and a conserved binding motif for SH3 domain-containing proteins indicated by asterisks. The GTPase domain (amino acids 55–324) is marked by arrows and the consensus sequence motifs for GTP binding at amino acids 55–63, 112–115, and 194–197 by lines. (B) Structure of variant human septin 3 transcripts. The open reading frame is shown by an open box and sequences corresponding to expressed sequence tags are indicated. The position of a highly repetitive tar-1-element, which seems to be translated in mouse sep3 is shown in relationship with the presumed open reading frame. (C) Approximate position of primers and probes. The approximate position of primers and probes used (forward primers F1–3 and reverse primers R1–3) is shown in relation to sep 3A.

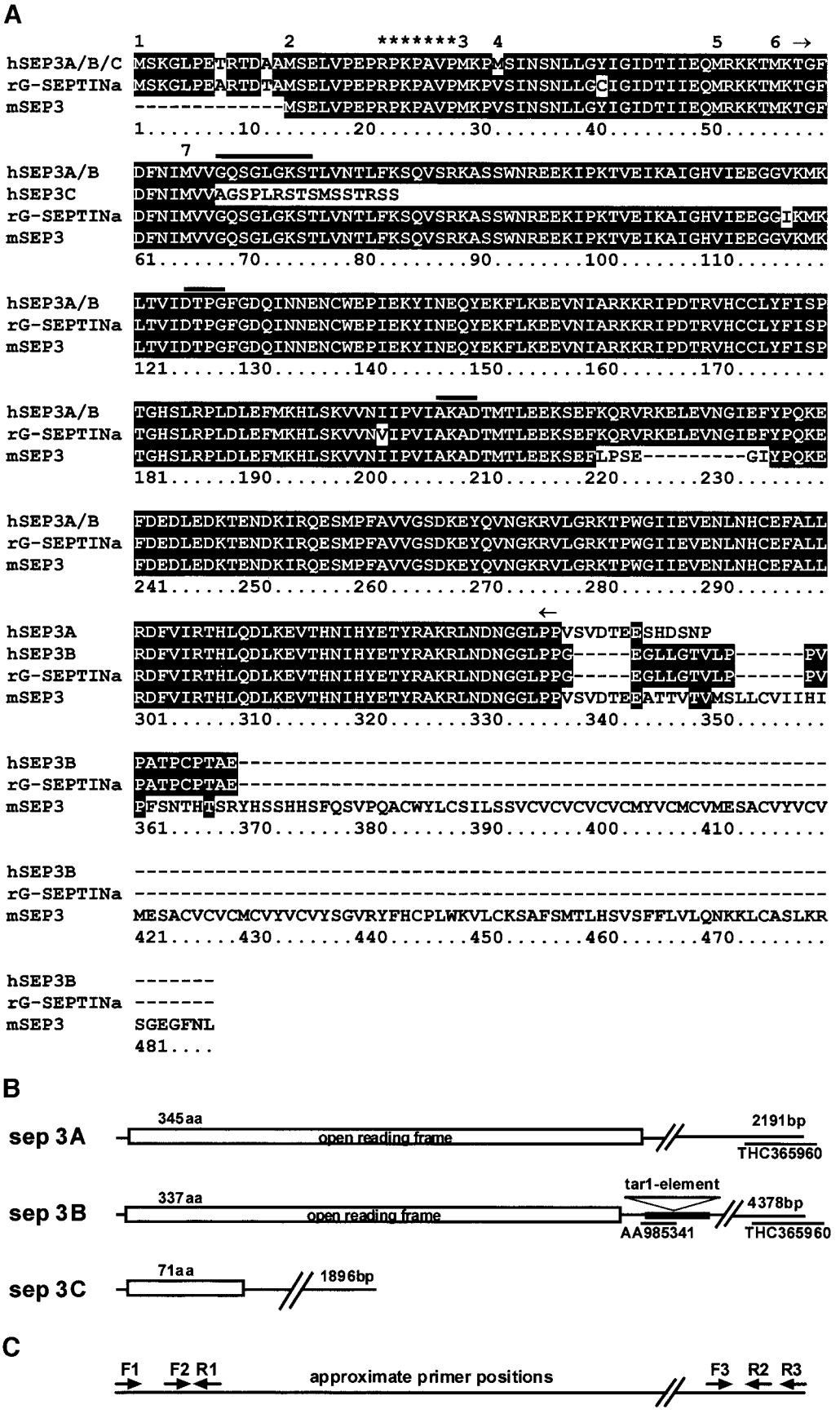
A
hSEP3A/B/C
rG-SEPTINa
mSEP3
hSEP3A/B
hSEP3C
hSEP3A
hSEP3B
B
sep 3A
345aa
open reading frame
2191bp
THC365960
sep 3B
337aa
tar1-element
4378bp
AA985341
sep 3C
71aa
1896bp
C
F1
F2
R1
approximate primer positions
F3
R2
R3

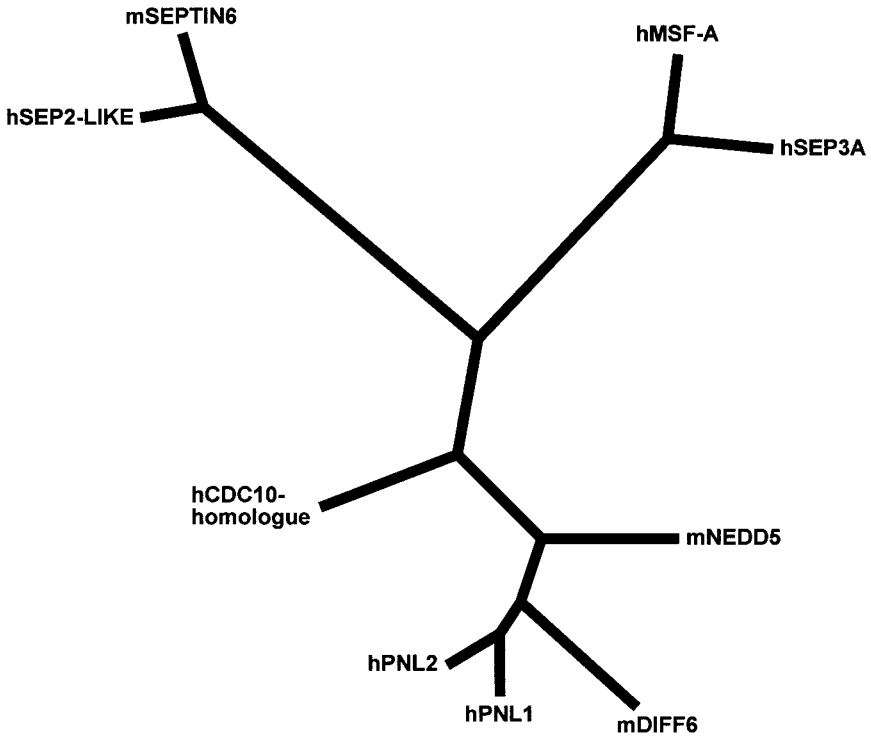

FIG. 3. Phylogenetic analysis of mammalian septins. Amino acid sequences of all available mammalian septins were aligned and a phylogenetic tree inferred by calculating maximum likelihood distances with Puzzle 5.0. The human ortholog was chosen where several mammalian sequences were available. All branch points were supported with a 100% reliability. Sequences used were human peanut-like protein 1 (hPNL1, alternative name: CDCREL-1), human peanut-like protein 2 (hPNL2, alternative name: brain protein H5), human CDC10 protein homolog, human MLL septin-like fusion protein (hMSF-A), human septin 2-like cell division control protein (hSEP2-LIKE), mouse DIFF6, mouse neural precursor cell expressed, developmentally down-regulated gene 5 (mNEDD5) and mouse septin6.

mouse neuronal-specific septin 3 (10) and rat brain-specific G-septin (11). The gene was named human septin 3 (sep3) in accordance with the HUGO Nomenclature Committee (www.gene.ucl.ac.uk/nomenclature). The presumed translated 5′ region of sep3 was identified by homology to the putative murine orthologs and the sequence information used to amplify the missing 5′ end from a human GeneFinder cDNA pool. The presumed full length sequence information was then used to amplify three specific PCR products of 1896 bp (sep 3C, GenBank Accession No. AF285108), 2191 bp (sep 3A, AF285107), and 4378 bp (sep 3B, AF285109) containing I-U#19 from cDNA derived from differentiated NT2 cells.

Prediction of Protein Structure and Function

The first 217 bp are identical in all three isoforms and include an start-ATG not preceded by a stop codon and six in frame ATGs within the first 210 bp. Only ATG #7 (Fig. 2A) resides in an appropriate context for translation initiation (37), but the sequence from ATG #2 downstream is conserved in man, mouse and rat, suggesting that the cloned sequence corresponds to the full length sequence. The 13 amino acids found upstream of ATG#2 in the rat homolog and in SEP3 do not show any homology to other septins, therefore we chose the conserved ATG #2 as start methionine. The open reading frame downstream from ATG #2 has 1037 bases (sep 3A), 1013 bases (sep 3B), and 212 bases (sep 3C) encoding polypeptides of 345, 337, and 71 amino acids, respectively. Sep 3A and Sep 3B differ in their C-terminal part and Sep 3C shares only the first 54 amino acids with the other isoforms (Fig. 2B). A data base search revealed that SEP3 is the probable human ortholog of rat G-SEPTIN and mouse neuronal-specific SEP3 with almost 100% sequence identity and that it shares similarities with other yeast, mammalian, and *Drosophila* septins. Like other septins, SEP3A and SEP3B contain a set of consensus sequence motifs for GTP binding at amino acids 55–63, 112–115, and 194–197 (Fig. 2A). These regions are highly conserved in the septin family of proteins, but are not found in other GTPase subfamilies (38) and are absent from SEP3C, which makes SEP3C an atypical member of this family or possibly a splicing artefact (see below). In contrast to most other mammalian septins, SEP3 does not contain a predicted coiled-coil domain at the C terminus. SEP3A and B contain two predicted phosphorylation sites for PKG (39) Thr^{42} and Ser^{78} as described for G-septin (11) and a conserved binding motif for SH3 domain-containing proteins. The mouse SEP3 contains

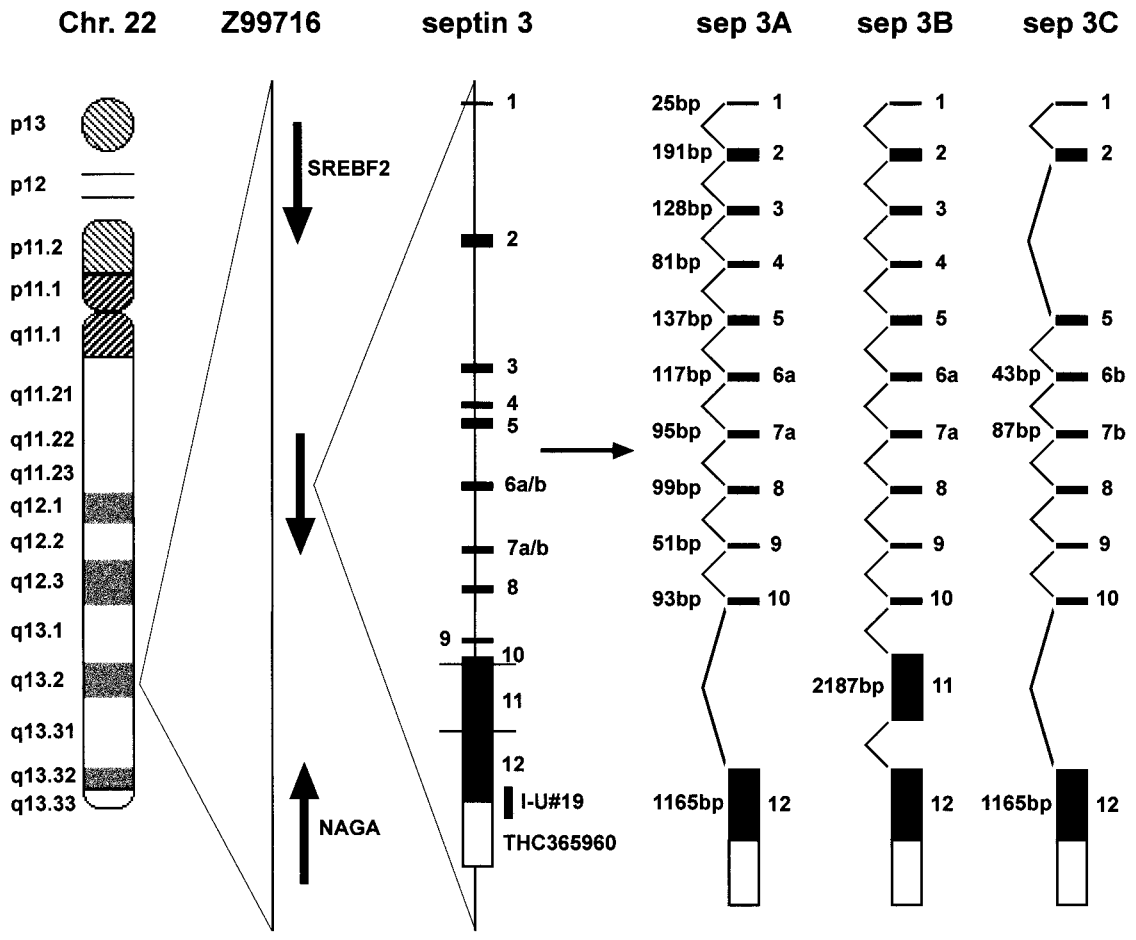

FIG. 4. Chromosomal organization of septin 3. Genes are indicated by arrows (SREBF2, sterol regulatory element binding transcription factor 2; NAGA, *α-N*-acetylgalactosaminidase) and exons by boxes. The open box corresponds to presumed transcribed sequence derived from the consensus expressed sequence tag THC365960. The location of I-U#19 is shown. The splicing events leading to the three isoforms sep3A, sep3B and sep3C are shown on the right side and the size of the presumed exons is indicated.

a highly hydrophobic domain at its C terminus distinct from other septins, which stems from the translation of a repetitive sequence also present, but not translated in human sep3B. In contrast to the mouse isoform this sequence is terminated in sep3B by a stop codon after 13 amino acids making the mouse protein unique among the three known mammalian SEP3 orthologs. The amino acid sequence of SEP3A and B was aligned with all known mammalian septins and an unrooted phylogenetic tree inferred from this alignment to elucidate their evolutionary relationship (Fig. 3). This analysis indicated that the nine mammalian septins fall into four groups comprising (i) hMSF-A and hSEP3; (ii) hSEP2-like and mSEPTIN6; (iii) hPNL1, hPNL2, mDIFF6, mNEDD5; and (iv) hCDC10-homolog. Human MSF (MLL septin-like fusion) is the most related septin with 71% amino acid identity. MSF was identified as a fusion partner of the MLL gene in a therapy-related acute myeloid leukemia (27). MLL is located on chromosome 11q23 and is frequently rearranged by chromosome translocations in *de novo* leukemias and in therapy-related leukemias. Of the 19 partner genes identified to date another septin, human peanut-like protein 1 (alternative name CDCrel-1), was found to be fused to MLL in infant twins suffering from leukemia (40).

Determination of Genomic Localization and Organization of Septin 3 on Chromosome 22q13.2

The genomic clone Z99716 harboring human sep3 maps to chromosome 22q13.2. The gene for sep3 is situated between the genes for sterol regulatory element binding transcription factor 2 towards the centromer and *α-N*-acetylgalactosaminidase towards the telomer of the chromosome. Interestingly, 125 chromosomal abberations involving chromosome 22q13 and acute or chronic leukemias have been described to date (http://cgap.nci.nih.gov/Chromosomes/Mitelman) (41), making the investigation of a possible involvement of SEP3 in these cases worthwhile. Sequence comparison of sep3A-C with z99716 identified twelve exons ranging from 25 to

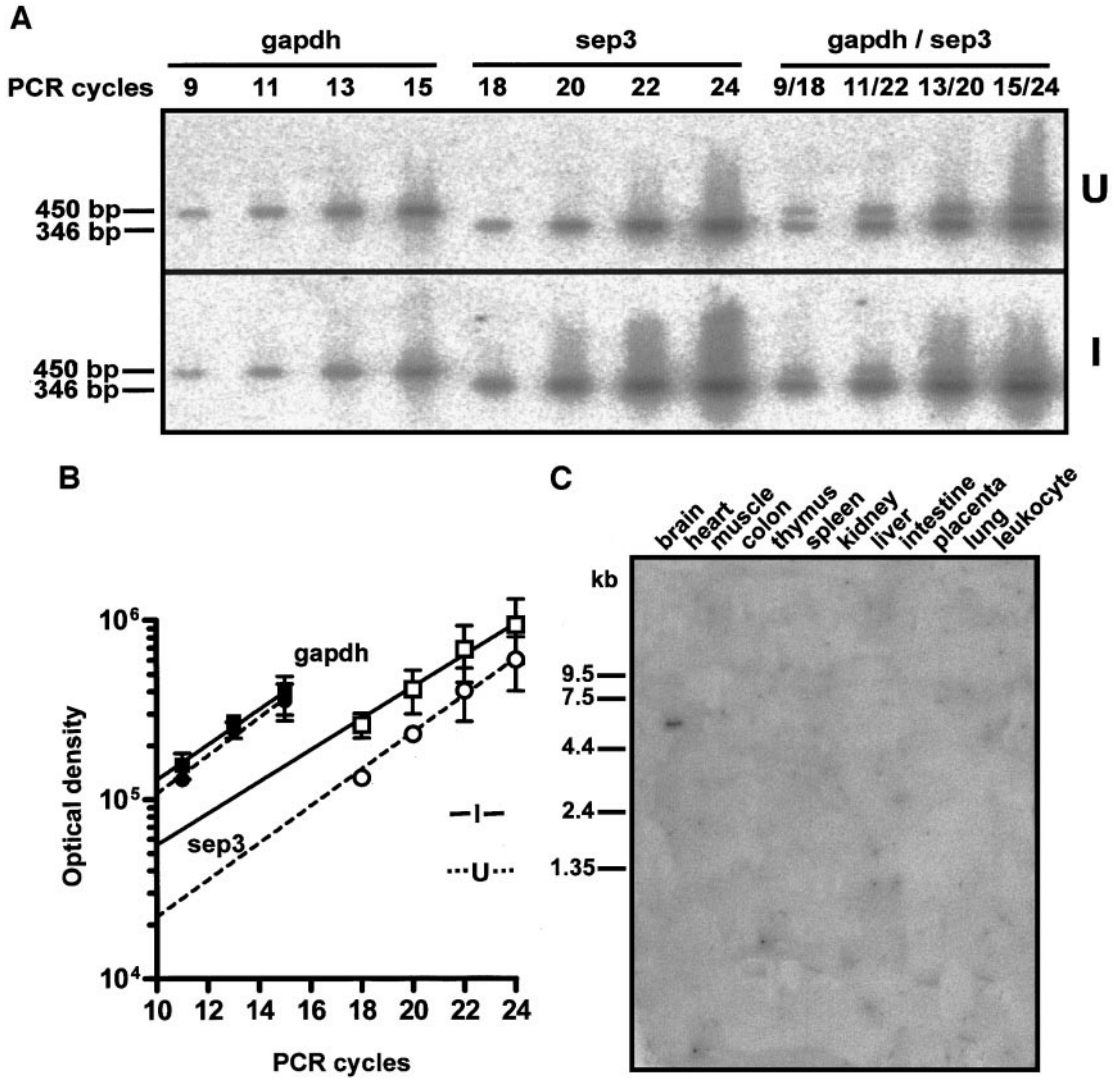

FIG. 5. Expression analysis of sep 3. (A) Quantitative PCR of sep3 on cDNA from induced and uninduced NT2 cells. Quantitative PCR containing either sep3 primers, gapdh primers as controls or both (multiplex PCR) on cDNA from induced (I) and uninduced (U) NT2 cells. Aliquots of each reaction were removed at the indicated cycle numbers and blotted after electrophoresis. Blots were hybridized with end-labeled oligonucleotides specific for sep3 and gapdh, washed under high stringency conditions and analyzed using a phosphoimaging system. Expected sizes of PCR products are indicated. (B) Control (gapdh) and sep3 reactions are in the exponential phase of amplification. A density profile was created for each lane in Fig. 2A. The optical density of each band was determined by calculating the area under the curve and plotted on a semi-logarithmic scale against the cycle number of each aliquot. Closed symbols, gapdh; open symbols, sep3; square and solid line, cDNA from uninduced NT2 cells (U); circle and dashed line, cDNA from induced NT2 cells (I). (C) Northern blot analysis of sep3 expression in human tissues. A human multiple tissue northern was purchased from Clontech, hybridized with a specific I-U#19 probe and washed under high stringency conditions.

2187 bp (Fig. 4). All intron junction sequences contained the highly conserved splice donor GT and splice acceptor AG dinucleotides (42). Sep3A and B differ only in the splicing of exon 11. The omission of exon 11 in sep3A leads to translation of 21 different C-terminal amino acids from exon 12. Exon 11 contains coding sequence for thirteen alternative amino acids in SEP3B, a tar1 repetitive element and part of the 5′ untranslated region. Sep3C differs substantially from the other two isoforms. Exons three and four are spliced out, which leads to a frame shift in exon five and a stop after 84 amino acids. Use of a cryptic splice donor site 5′-AAG_GTTGTG-3′ in exon 6b, where the underlined sequence does not comply with the consensus sequence (42) and a different splice acceptor site in exon 7b leads to smaller exons without coding information. Exon 11 is spliced out in sep3C as in sep3A.

Septin 3 Is Specific for Neuronal Tissues

Sep3 was found by quantitative PCR to be upregulated two-fold (Figs. 5A and 5B) in cDNA from induced

NT2 cells (SEM 0.1698, $P < 0.005$). Northern blot analysis was performed to determine the tissue distribution of mRNA encoding septin 3. A transcript of 5 kb was detected only in adult brain (Fig. 5C), but not in other tissues such as adult human heart, skeletal muscle, colon, thymus, spleen, kidney, liver, small intestine, placenta, lung, and leukocytes. Therefore, from the size we deduce, that the sep3B transcript seems to be the predominant isoform, at least in the tissues examined. The brain-specific expression confirms the results from induced NT2 cells. It is tempting to speculate that the relative small difference in expression found by the quantitative PCR experiments might be due to the fact, that the induced NT2 cells are not pure postmitotic neurons, but a mixture of neuronal cells and uncharacterized cells residing in the aggregates.

A number of other septins are also found in postmitotic neurons. High levels of *Drosophila* SEP1 were found in central and peripheral nervous tissue (43), and PNUT was also observed in *Drosophila* neural tissue (17). CDCrel-1 is brain-specific in rats; SEPTIN 3/G-SEPTIN, CDC10, H5, and NEDD5 are abundant in brain. NEDD5, H5, DIFF6 were identified in neurofibrillary tangles in brains affected by Alzheimer's disease (44) and also in fine fibrillar deposits in neuronal soma, which are considered the earliest detectable stages of neurofibrillary tangle formation. These findings suggest that septins may have a function in the etiology of neuronal disease. Neuronal septins probably do not play a role in cytokinesis since neurons in adult brain generally do not divide. New roles for neuronal septins are emerging in synaptic transmission. Four septins have been identified in a protein complex that can interact with the SEC6-SEC8 complex in rat brain and that can assemble as filaments. Since the SEC6-SEC8 complex is a cluster of molecules essential for exocytosis, septins may have a role that links the secretory machinery to the actin-based cytoskeleton beneath the plasma membrane (45). The brain-specific human peanut-like protein 1 (CDCrel-1) and the more widely expressed NEDD5 proteins have been shown to be essential for exocytosis in neurons (19). Both proteins immunoprecipitated with the *N*-ethylmaleimide-sensitive factor attachment protein receptor (SNARE) protein syntaxin, and transfection of wild-type or dominant-negative mutants of human CDCrel-1 inhibited or enhanced, respectively, exocytosis from cultured neuroendocrine cells. The possible role of SEP3 in neurons can in part be deducted from the studies made in the murine homologs. Mouse neuronal-specific septin 3 was found to be upregulated in neuronal tissue during development (10) and the highly homologous rat G-SEPTIN has been implicated in the modulation of neuronal function by specific phosphorylation involving type I cGMP-dependent protein kinase (11). The human model system for neuronal differentiation used in this study, RA induced differentiation of the neuronal precursor cell line NT2, seems to be a suitable tool to examine the role of septin 3 in human tissues.

ACKNOWLEDGMENTS

We are most grateful for the continuous support and the laboratory space provided by Prof. Dr. Chica Schaller. This work was funded by the Deutsche Forschungsgemeinschaft within the Graduiertenkolleg 255.

REFERENCES

1. Pleasure, S. J., and Lee, V. M. (1993) NTera 2 cells: A human cell line which displays characteristics expected of a human committed neuronal progenitor cell. *J. Neurosci. Res.* **35,** 585–602.
2. Horton, C., and Maden, M. (1995) Endogenous distribution of retinoids during normal development and teratogenesis in the mouse embryo. *Dev. Dyn.* **202,** 312–323.
3. Rossant, J., *et al.* (1991) Expression of a retinoic acid response element-hsplacZ transgene defines specific domains of transcriptional activity during mouse embryogenesis. *Genes Dev.* **5,** 1333–1344.
4. Wagner, M., Han, B., and Jessell, T. M. (1992) Regional differences in retinoid release from embryonic neural tissue detected by an in vitro reporter assay. *Development* **116,** 55–66.
5. Maden, M., Ong, D. E., and Chytil, F. (1990) Retinoid-binding protein distribution in the developing mammalian nervous system. *Development* **109,** 75–80.
6. Ruberte, E., *et al.* (1993) Retinoic acid receptors and cellular retinoid binding proteins. III. Their differential transcript distribution during mouse nervous system development. *Development* **118,** 267–282.
7. Lyn, S., and Giguere, V. (1994) Localization of CRABP-I and CRABP-II mRNA in the early mouse embryo by whole-mount in situ hybridization: Implications for teratogenesis and neural development. *Dev. Dyn.* **199,** 280–291.
8. Zetterstrom, R. H., *et al.* (1999) Role of retinoids in the CNS: Differential expression of retinoid binding proteins and receptors and evidence for presence of retinoic acid. *Eur. J. Neurosci.* **11,** 407–416.
9. Leypoldt, F., Lewerenz, J., and Methner, A. (2001) Identification of Genes upregulated by retinoic acid induced differentiation of the human neuronal precursor cell line Ntera2cl.D/1. *J. Neurochem.* **76,** 806–814.
10. Xiong, J. W., Leahy, A., and Stuhlmann, H. (1999) Retroviral promoter-trap insertion into a novel mammalian septin gene expressed during mouse neuronal development. *Mech. Dev.* **86,** 183–191.
11. Xue, J., *et al.* (2000) Phosphorylation of a new brain-specific septin, G-septin, by cGMP-dependent protein kinase. *J. Biol. Chem.* **275,** 10047–10056.
12. Hartwell, L. H. (1971) Genetic control of the cell division cycle in yeast. IV. Genes controlling bud emergence and cytokinesis. *Exp. Cell Res.* **69,** 265–276.
13. Saraste, M., Sibbald, P. R., and Wittinghofer, A. (1990) The P-loop—A common motif in ATP- and GTP-binding proteins. *Trends Biochem. Sci.* **15,** 430–434.
14. Byers, B., and Goetsch, L. (1976) A highly ordered ring of membrane-associated filaments in budding yeast. *J. Cell Biol.* **69,** 717–721.
15. Longtine, M. S., *et al.* (1996) The septins: Roles in cytokinesis and other processes. *Curr. Opin. Cell Biol.* **8,** 106–119.
16. Field, C. M., *et al.* (1996) A purified Drosophila septin complex

forms filaments and exhibits GTPase activity. *J. Cell Biol.* **133,** 605–616.

17. Neufeld, T. P., and Rubin, G. M. (1994) The Drosophila peanut gene is required for cytokinesis and encodes a protein similar to yeast putative bud neck filament proteins. *Cell* **77,** 371–379.
18. Kinoshita, M., *et al.* (1997) Nedd5, a mammalian septin, is a novel cytoskeletal component interacting with actin-based structures. *Genes Dev.* **11,** 1535–1547.
19. Beites, C. L., *et al.* (1999) The septin CDCrel-1 binds syntaxin and inhibits exocytosis. *Nat. Neurosci.* **2,** 434–439.
20. Nottenburg, C., Gallatin, W. M., and St. John, T. (1990) Lymphocyte HEV adhesion variants differ in the expression of multiple gene sequences. *Gene* **95,** 279–284.
21. Kato, K. (1992) Finding new genes in the nervous system by cDNA analysis. *Trends Neurosci.* **15,** 319–323.
22. Nakatsuru, S., Sudo, K., and Nakamura, Y. (1994) Molecular cloning of a novel human cDNA homologous to CDC10 in Saccharomyces cerevisiae. *Biochem. Biophys. Res. Commun.* **202,** 82–87.
23. McKie, J. M., *et al.* (1997) A human gene similar to Drosophila melanogaster peanut maps to the DiGeorge syndrome region of 22q11. *Hum. Genet.* **101,** 6–12.
24. Zieger, B., Hashimoto, Y., and Ware, J. (1997) Alternative expression of platelet glycoprotein Ib (beta) mRNA from an adjacent 5′ gene with an imperfect polyadenylation signal sequence. *J. Clin. Invest.* **99,** 520–525.
25. Nagase, T., *et al.* (1995) Prediction of the coding sequences of unidentified human genes. IV. The coding sequences of 40 new genes (KIAA0121-KIAA0160) deduced by analysis of cDNA clones from human cell line KG-1. *DNA Res.* **2,** 167–174, 199–210.
26. Nagase, T., *et al.* (1999) Prediction of the coding sequences of unidentified human genes. XIII. The complete sequences of 100 new cDNA clones from brain which code for large proteins in vitro. *DNA Res.* **6,** 63–70.
27. Osaka, M., Rowley, J. D., and Zeleznik-Le, N. J. (1999) MSF (MLL septin-like fusion), a fusion partner gene of MLL, in a therapy-related acute myeloid leukemia with a t(11;17)(q23;q25). *Proc. Natl. Acad. Sci. USA* **96,** 6428–6433.
28. Sorensen, A. B., *et al.* (2000) Sint1, a common integration site in SL3-3-induced T-cell lymphomas, harbors a putative proto-oncogene with homology to the septin gene family [In Process Citation]. *J. Virol.* **74,** 2161–2168.
29. Cheung, W. M., *et al.* (1999) Production of human CNS neurons from embryonal carcinoma cells using a cell aggregation method. *Biotechniques* **26,** 946–948, 950–952, 954.
30. Altschul, S. F., *et al.* (1990) Basic local alignment search tool. *J. Mol. Biol.* **215,** 403–410.
31. Horowitz, D., and Kraier, A. (1994) Mechanisms for selecting 5′ splice sites in mammalian pre-mRNA splicing. *Trends Genet.* **10,** 100–106.
32. Thompson, J. D., Higgins, D. G., and Gibson, T. J. (1994) CLUSTAL W: Improving the sensitivity of progressive multiple sequence alignment through sequence weighting, positions-specific gap penalties and weight matrix choice. *Nucl. Acids Res.* **22,** 4673–4680.
33. Strimmer, K., *et al.* (1996) Quartet puzzling: A quartet maximum likelihood method for reconstructing tree topologies. *Mol. Biol. Evol.* **13,** 964–969.
34. Jones, D. T., *et al.* (1992) The rapid generation of mutation data matrices from protein sequences. *Cabios* **8,** 275–282.
35. Smith, S. C., *et al.* (1987) The role of aggregation in embryonal carcinoma cell differentiation. *J. Cell Physiol.* **131,** 74–84.
36. Larue, L., *et al.* (1996) A role for cadherins in tissue formation. *Development* **122,** 3185–3194.
37. Kozak, M. (1984) Compilation and analysis of sequences upstream from the translational start site in eukaryotic mRNAs. *Nucleic Acid Res.* **12,** 857–870.
38. Bourne, H. R., Sanders, D. A., and McCormick, F. (1991) The GTPase superfamily: Conserved structure and molecular mechanism. *Nature* **349,** 117–127.
39. Tegge, W., *et al.* (1995) Determination of cyclic nucleotide-dependent protein kinase substrate specificity by the use of peptide libraries on cellulose paper. *Biochemistry* **34,** 10569–10577.
40. Megonigal, M., *et al.* (1998) t(11;22)(q23;q11.2) In acute myeloid leukemia of infant twins fuses MLL with hCDCrel, a cell division cycle gene in the genomic region of deletion in DiGeorge and velocardiofacial syndromes. *Proc. Natl. Acad. Sci. USA* **95,** 6413–6418.
41. Mitelman, F., Johansson, B., and Mertens, F. (2001) Mitelman Database of Chromosome Aberrations in Cancer.
42. Senapathy, P., Shapiro, M. B., and Harris, N. L. (1990) Splice junctions, branch point sites, and exons: Sequence statistics, identification, and applications to genome project. *Methods Enzymol.* **183,** 252–278.
43. Fares, H., Peifer, M., and Pringle, J. R. (1995) Localization and possible functions of Drosophila septins. *Mol. Biol. Cell* **6,** 1843–1859.
44. Kinoshita, A., *et al.* (1998) Identification of septins in neurofibrillary tangles in Alzheimer's disease. *Am. J. Pathol.* **153,** 1551–1560.
45. Hsu, S. C., *et al.* (1998) Subunit composition, protein interactions, and structures of the mammalian brain sec6/8 complex and septin filaments. *Neuron* **20,** 1111–1122.